ORIGINAL ARTICLE

Histological Reaction to Porous Coral and Ceramic Bone

Takanao ONO[1], Tetsunari NISHIKAWA[2], Akio TANAKA[2]
and Naoyuki MATSUMOTO[1]

[1]Department of Orthodontics, [2]Department of Oral Pathology,
Osaka Dental University, Osaka, Japan

SYNOPSIS

There are many reports on the induction of new bone with synthetic bone substitutes. However, the histological reaction to scaffold, are still not completely understood. In this study we clarified the the effects on capillary differentiation and the mechanisms of bioabsorption in coral and artificial hydroxyapatite ceramic bone (ceramic bone), both of which have porous structures. The micromorphology of both coral and ceramic bone was observed by SEM, and their compressive strength was measured. *In vitro*, normal human dermal fibroblasts and human umbilical vein endothelial cells were co-cultured with added particles of coral and ceramic bone in experimental groups. Meanwhile, no particles were added in a control group. After co-culturing for 14 days, cell proliferation was observed with DAPI nuclear stain and capillary formation was observed with anti-human CD31 antibodies in the experimental and control groups. Next, *in vivo*, coral and ceramic bone particles were implanted in the dorsal subcutaneous tissue of rats, and the bioabsorption process of the respective particles was observed histologically. The coral had a porous structure with numerous tubes of 50-300 µm in diameter with interconnection pathways of 50-100 µm, and the ceramic bone had a porous structure with spherical pores of 100-200 µm with interconnection pathways of 15-50 µm. The compressive strength of coral was higher than that of ceramic bone. *In vitro*, cell proliferation and formation of capillaries were seen adjacent to the added coral and ceramic bone particles. *In vivo*, all the implanted coral and ceramic bone particles remained after 2 weeks, and many were seen to be enclosed by granulation tissue. After 4 and 6 weeks, replacement of particles by granulation tissue and phagocytosis of particles by foreign body giant cells were observed. At 8 and 12 weeks, many cases of particle disappearance were seen in the coral group, and coral particles were replaced with fibrous connective tissue. In the ceramic bone group, there were few cases of particle disappearance. These findings suggest that the porous structures of both coral and ceramic bone induce cell proliferation and capillary formation. Coral particles have greater compressive strength and bioabsorbability than ceramic bone.

Key words: *coral, ceramic bone, tissue affinity, capillary differentiation, bioabsorption*

INTRODUCTION

Bone augmentation is desirable to improve esthetics or occlusal function in hypoplastic growth of the maxilla or bone resorption due to periodontal diseases, cystic diseases, tumors, or other causes. For bone regeneration to occur, cells (osteoblasts and osteoclasts), osteogenic growth factors, and scaffolding are needed [1]. Advances in the scaffold for bone defects require temporal distribution of the scaffold and cells compatible with enhanced bone healing. To meet functional demands, materials with desired physical, chemical, and biological, properties must be selected [2]. Then new bone needs to be induced, and finally this new bone needs to replace the scaffold [3]. Physical strength is needed in scaffolding for bone augmentation to withstand the pressure from surrounding tissue and to secure sufficient space for the formation of new bone [4, 5].

In cases of mandibular reconstruction or large bone defects from removal of tumors or cysts, bone defects are filled with autogenous bone grafts harvested from the patients [6, 7]. Such autogenous bone grafts are the most promising in bone regeneration [8]. However, this method involves a high level of patient invasiveness and the amount of bone that can be harvested is limited [9]. In place of autogenous bone, therefore, application of synthetic bone grafts has been conducted [10-12]. Porous, interconnected structures with rough surfaces are thought to be ideal in the formation of new bone and the formation of capillaries that are needed for bone formation [13-15].

Feng *et al*. (2012) [16] used tubular β-TCP blocks in large defects in rabbits and reported that they were effective in bone regeneration. Mastrogiacomo *et al*. (2006) [17] applied ceramic bone to defects in sheep and reported seeing formation of new bone in interconnection

pathways. As seen above, there are many reports on the induction of new bone with synthetic bone substitutes [18, 19]. However, the histological response to scaffold, particularly the induction of differentiation to capillaries that is necessary for new bone formation, and absorption of materials by the host, are still not completely understood.

We examined the effects on the host in response to coral and ceramic bone scaffolding, which meet the needs for porosity and physical strength, by clarifying the cell affinity and differentiation into capillaries *in vitro* and bioabsorption *in vivo*, and demonstrated the histological response to each of these scaffoldings.

MATERIALS AND METHODS
1. Materials

Coral (*Porites Cylindrica*) provided by Professor Michio Hidaka of the Faculty of Science, University of the Ryukus, was immersed in 1 N sodium hydroxide under vacuum (20 hPa) to eliminate protein. The artificial ceramic bone used was porous hydroxyapatite (Neo Bone®, Covalent Materials Corporation, Tokyo, Japan). These particles were divided by size into a small group: 100–300 μm, medium group: 300–500 μm, and large group: 500–800 μm in the coral and ceramic bone groups, respectively. After neutralizing by immersion in 0.01 M phosphate buffered saline (PBS, pH 7.2), they were sterilized in an autoclave (121°C, 20 min, 1.2 atmospheres)

2. Observation of surface microstructure

After vapor deposition of platinum and palladium using an ion coater (Ion Sputter, E-1030, Hitachi, Tokyo, Japan), the surface micromorphology of the coral and ceramic bone were observed with a scanning electron microscope (SEM, S-4000, Hitachi).

3. Measurements of compressive strength

Cylindrical blocks (*n*=8, 3 mm in diameter and 5 mm in high) of the coral and ceramic bone were prepared with a diamond saw (EXACT Appararebau Gmblt Moiwa, Osaka, Japan). The compressive strength of both blocks was measured using a universal testing machine (Imada Seisakusho Co. Ltd, Aichi, Japan), and converted to units of MPa from kgf/cm^2. Statistical differences of *p*>0.05 by two-sided Student's *t*-test were considered significant.

4. Tissue affinity and differentiation into capillaries *in vitro*

Normal human dermal fibroblasts (NHDF) and human umbilical vein endothelial cells (HUVEC) were seeded in a 24-well plate (Angiogenesis Kit, IKZ-1000, Kurabo, Osaka, Japan) and co-cultured in an incubator (TABAI ESPEC, BNA-1121D, Osaka, Japan) at 37°C in a humidified atmosphere containing 5% CO_2.

Particles of coral and ceramic bone (small group: 100–300 µm, medium group: 300–500 µm, large group: 500–800 µm) were added as experimental group, while no particles were added in a control group. After co-culturing for 14 days, samples were fixed with 80% ethanol and stained with DAPI nuclear fluorescent stain (a shield mounting medium with DAPI, Vector, Tokyo, Japan). Cell proliferation was then observed with a fluorescence microscope (BZ-9000, Keyence, Osaka, Japan).

After blocking endogenous peroxidase by autoclaving for 15 min at 121°C in PBS containing 0.3% hydrogen peroxide solution, non-specific reactions were blocked with PBS containing 3% bovine serum albumin (Dako Cytomation, Carpinteria, California, USA) for 30 min. Next, co-cultured cells were allowed to react with anti-human CD31 mouse monoclonal antibodies (Tubule Staining Kit, Kurabo), a marker of vascular endothelial cells, in a primary reaction. These cells were secondarily reacted with alkaline phosphatase-labeled anti-mouse IgG goat antibody and colored with 5-bromo-4-chloro-3-indoxy phosphate/nitro blue terazolium (BCIP/NBT), or with FITC-labeled anti-mouse IgG antibodies (polyclonal rabbit, Dako Cytomation, Giostrup, Denmark). Anti-human CD31 positive cells were then observed with a fluorescence microscope (BZ-9000, Keyence, Osaka, Japan), and the formation of capillaries was compared in the experimental and control groups.

5. Bioabsorbability *in vivo*

Coral and ceramic bone particles (small group: 100–300 µm, medium group: 300–500 µm, large group: 500–800 µm), respectively, were mixed with propylene glycol and deaerated in a vacuum (20 hPa). 44 male Wistar rats (5 weeks old) were then given peritoneal injection of pentobarbital and local injection of lidocaine, incisions were made in their backs, and the particles were implanted in subcutaneous tissue. Propylene glycol alone was also implanted in the control group. Animals were euthanized with an overdose of pentobarbital general anesthetic at 2, 4, 6, 8, and 12 weeks after implantation. They were then perfusion fixed with saline and 10% formalin and the subcutaneous tissue was removed. Paraffin sections of this subcutaneous tissue were prepared following normal procedures, and stained with hematoxylin and eosin. Pathological observations of these sections were made under a light microscope (BX50, Olympus, Tokyo, Japan), and the processing of these particles by the body was investigated histologically. The processing of the particles by granulation tissue was divided into 3 types: an encapsulation type in which granula-

granulation tissue enclosed particle clusters, an organization type in which granulation tissue invaded, sequestered, and replaced particle clusters, and an encapsulation/organization type. At the same time, the remaining particle material was histologically analyzed according to the following 6 levels based on number of particles and the length of the major axis of particle clusters: (0) complete disappearance, (1) 1 or 2 particles, (2) >3 particles, (3) particle clusters of >1 mm in length, (4) >2 mm length, (5) >3 mm length. Statistical differentiation was determined using a two-sided Mann-Whitney's *U*-test. Differences of *P*<0.05 were considered significant. Lymphocytes, macrophages and foreign body giant cells in the granulation tissue were also observed, and the degree of infiltration by foreign body giant cells was divided into 3 types: (0) no giant cell infiltration, (1) 1 or 2 giant cells, (2) >3 giant cells on the surface and interconnection pathways of the particles.

This animal experiment using rats was approved by the Animal Experiment Committee of Osaka Dental University (No. 13-03001), and performed in accordance with animal experiment regulations. The number of animals was minimized, and intraoperative pain was minimized with the use of anesthesia.

RESULTS
1. Observation of surface microstructure
The internal structure of coral showed porosity with numerous tubes of various diameters from 50–300 µm. There were interconnection pathways of 50–100 µm (Fig. 1a, b). The exoskeleton surface was covered with rough elevations of 10–20 µm (Fig. 1c). The internal structure of the ceramic bone was a porous structure of nearly spherical pores of 100–200 µm, with interconnection pathways of 15–50 µm (Fig. 1d). The surface was also rough, but not as rough as the coral (Fig. 1e).
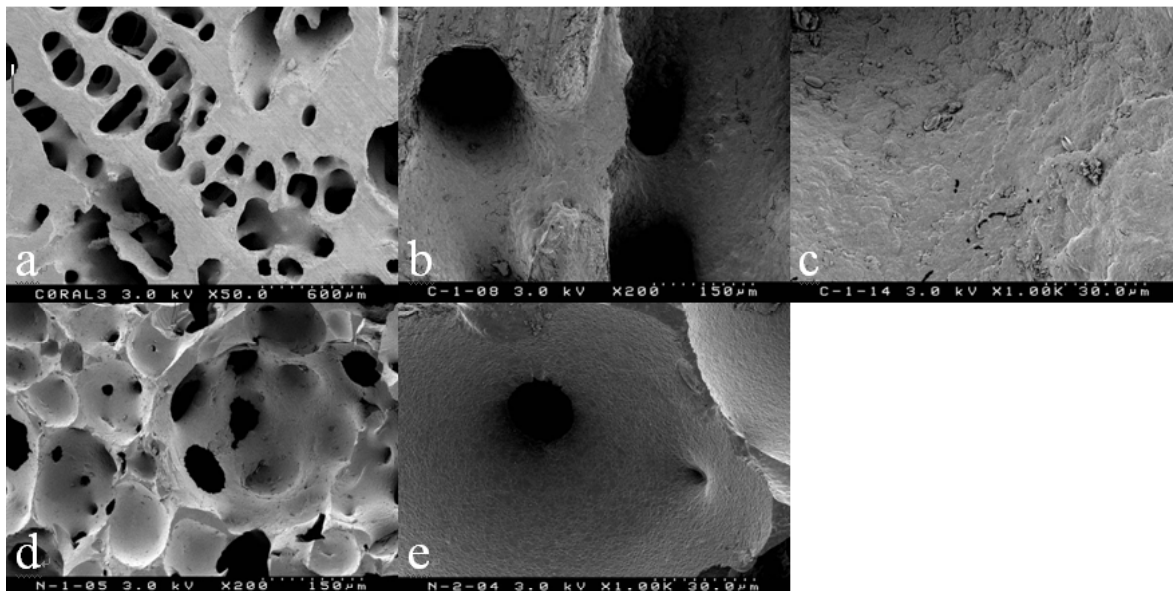

Fig. 1. SEM image of coral and ceramic bone.
ab. Longitudinal image of coral, c. Surface of coral exoskeleton, d. Longitudinal image of ceramic bone, e. Surface of ceramic bone.
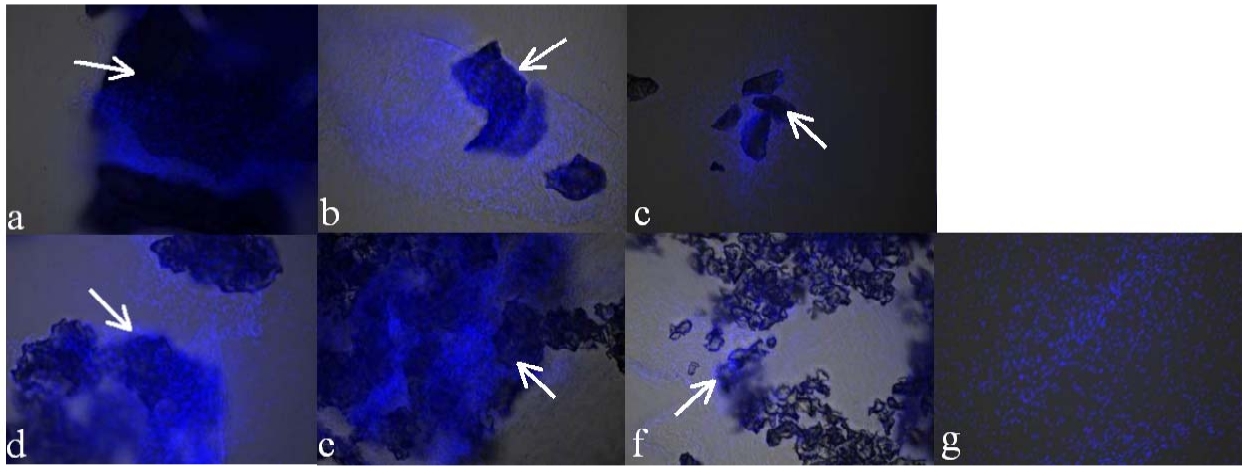
Fig. 2 Tissue affinity stained with DAPI nuclear stain (blue).
a. Large group of coral (arrow), b. Medium group of coral (arrow), c. Small group of coral (arrow), d. Large group of ceramic bone (arrow), e. Medium group of ceramic bone (arrow), f. Small group of ceramic bone (arrow), g. Control group.
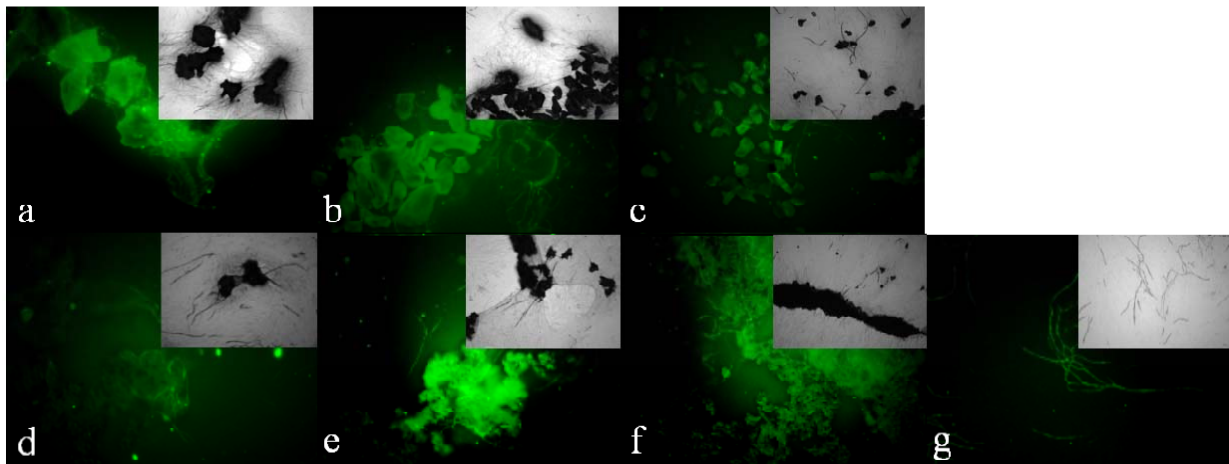

Fig. 3 Capillary differentiation stained with anti-human CD31 antibody and FITC (green), and BICP/NBT (black).
a. Large group of coral, b. Medium group of coral, c; Small group of coral, d. Large group of ceramic bone, e. Medium group of ceramic bone, f. Small group of ceramic bone, g. Control group.
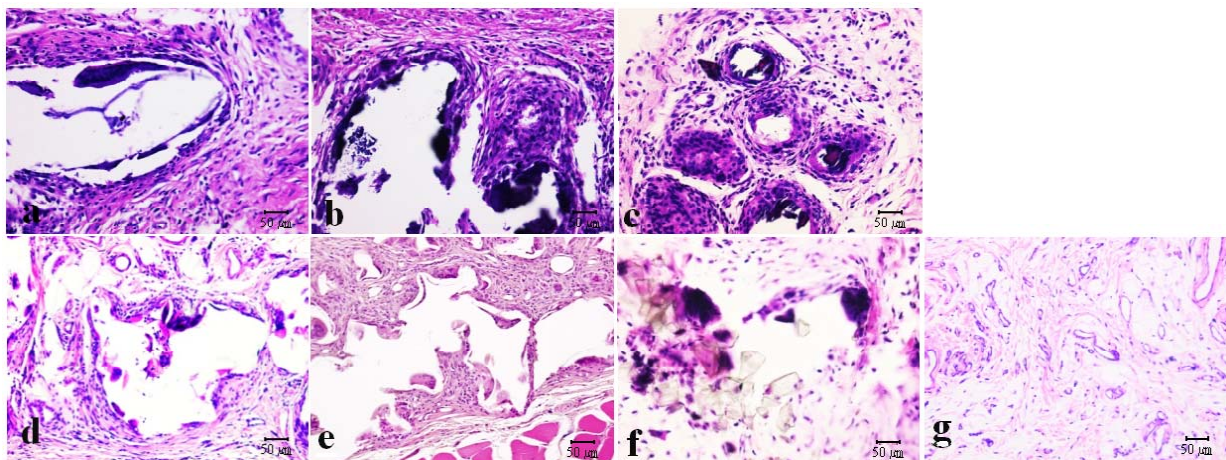

Fig. 4 Histological image of rat subcutaneous tissue (HE stain) 2 weeks after particles were implanted.
a. Large group of coral (encapsulation), b. Medium group of coral (encapsulation), c. Small group of coral (organization), d. Large group of ceramic bone (encapsulation), e. Medium group of ceramic bone (encapsulation/organization), f. Small group of ceramic bone (encapsulation), g. Control group.

2. Measurements of compressive strength

The compressive strength of both the coral and ceramic bone in a dry condition was 64.3 ± 12.5 MPa and 44.8 ± 9.5 MPa respectively, and that of the coral was significantly higher than that of the ceramic bone ($P<0.05$).

3. Tissue affinity and differentiation into capillary *in vitro*

In the large, medium and small particle of the coral experimental group, there were a few cells with nuclei positive for DAPI stain in places distant from the added particles, but proliferation of DAPI positive cells was observed mostly around the particles and in contact with the coral exoskeleton. (Figs. 2a, 2b, 2c). In the ceramic bone experimental group as well, there were a few DAPI positive cells in places distant from the added particles, but many DAPI positive cells were observed in contact with particles in the large, and medium and small groups (Figs. 2d, 2e, 2f). In the control group without added particles, uniform proliferation of DAPI positive cells was seen on the well plate surfaces (Fig. 2g).

In regard to capillary differentiation, there were fewer anti-human CD31 positive capillaries in places distant from the added particles in the coral experimental group than in the control group, but formation of many capillaries was seen around the particles or in contact with the particles (Figs. 3a, 3b, 3c). In the ceramic bone experimental group, there were fewer anti-human CD31 positive cells than in the control group in places distant from the added particles, but formation of many capillaries was seen around the added particles (Figs. 3d, 3e, 3f). In the control group, uniform formation of capillaries was observed on the well plate surfaces (Fig. 3g).

4. Bioabsorbability *in vivo*

2 weeks after implantation in the coral experimental group, the implanted par-ticles in the large, medium, and small groups remained, and the encapsulation type was seen more than the encapsulation/organization type or the organization type. Granulation tissues with capillaries, fibroblasts, and mild infiltration of lymphocytes, macrophages and foreign body giant cells were observed, but almost no neutrophils were seen in the large, medium, and small groups (Figs. 4a, 4b, 4c, 9, 10, 11). In the ceramic bone experimental group, the encapsulation type was more common in the large (50.0%), medium (50.0%), and small (62.5%) groups, and lymphocyte and macrophage infiltration was observed (Figs. 4d, 4e, 4f, 9, 10, 11). In the control group, no marked histological changes were observed other than mild capillary enlargement (Fig. 4g).

At 4 weeks after implantation, the organization type was more common in the large (57.2%), medium (57.2%) and small (85.8%) groups of the coral experiment group, and reduction of the area of the particle clusters was seen, particularly in small group. There was lymphocyte and macrophage infiltration in the granulation tissue, in addition to which infiltration and phagocytosis of particles by foreign body giant cells was observed and reduction of the area of the remaining particle clusters was seen in the large (26.8%), medium (26.8%), and small (71.4%) groups (Figs. 5a, 5b, 5c, 9, 10, 11). In the ceramic bone experimental group, the organization type was increased in the large, medium, and small groups. In addition to infiltration of lymphocytes, macrophages and foreign body giant cells with phagocytosis of particles in the granulation tissue was observed (Figs. 5d, 5e, 5f, 9, 10, 11). The number of cases with reduction of the area of the remaining particles statistically increased in the large, medium, and small groups of the coral group compared with the respective ceramic bone experimental group ($P<0.05$) (Fig. 10).
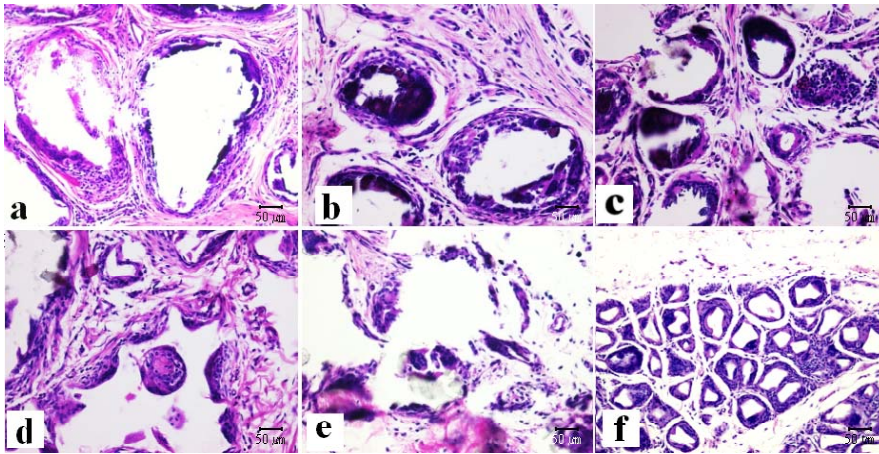
Fig. 5 Histological image of rat subcutaneous tissue (HE stain) 4 weeks after particles were implanted. a. Large group of coral (encapsulation/organization), b. Medium group of coral (encapsulation/organization), c. Small group of coral (organization), d. Large group of ceramic bone (encapsulation/organization), e. Medium group of ceramic bone (encapsulation/organization), f. Small group of ceramic bone (organization).
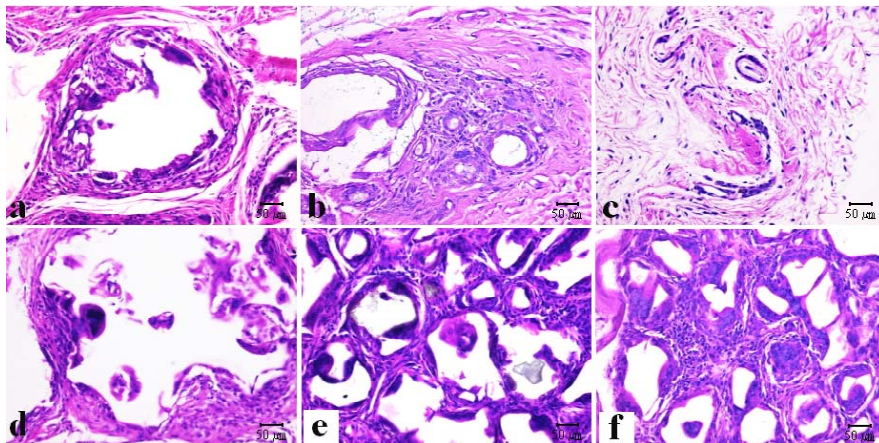

Fig. 6 Histological image of rat subcutaneous tissue (HE stain) 6 weeks after particles were implanted. a. Large group of coral (encapsulation/organization), b. Medium group of coral (organization), c. Small group of coral (disappearance), d. Large group of ceramic bone (encapsulation/organization), e. Medium group of ceramic bone (organization), f, Small group of ceramic bone (organization).
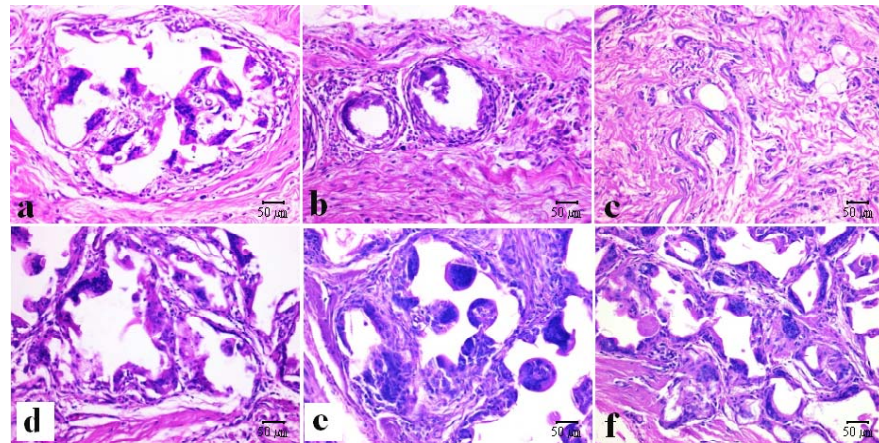

Fig. 7 Histological image of rat subcutaneous tissue (HE stain) 8 weeks after particles were implanted. a. Large group of coral (organization), b. Medium group of coral (organization), c. Small group of coral (disappearance), d. Large group of ceramic bone (organization), e. Medium group of ceramic bone (organization), f. Small group of ceramic bone (organization).

Fig. 8 Histological image of rat subcutaneous tissue (HE stain) 12 weeks after particles were implanted. a. Large group of coral (disappearance), b. Medium group of coral (disappearance), c. Small group of coral (disappearance), d. Large group of ceramic bone (organization), e. Medium group of ceramic bone (organization), f. Small group of ceramic bone (organization).
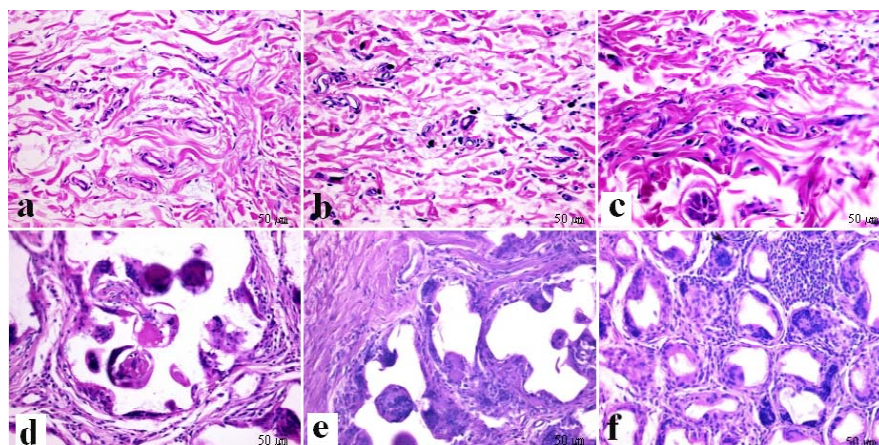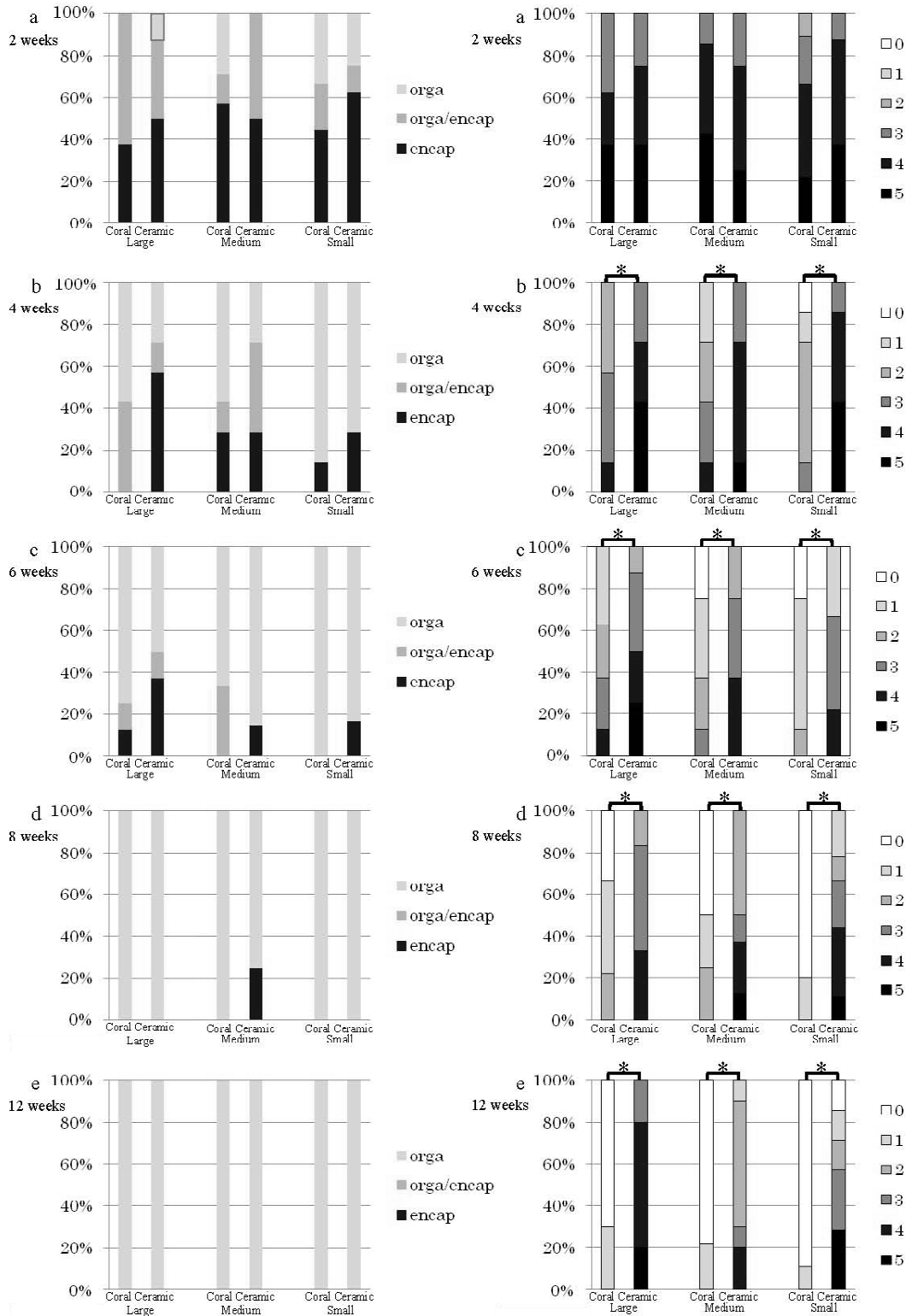
Fig.9 Types of particle processing by granulation tissue (coral and bioceramic bone). a; 2 weeks after implantation of particles (large group, medium group, and small group). b; 4 weeks, c; 6 weeks, d; 8 weeks, e; 12 weeks. The processing of the particles was divided into 3 types: an encapsulation type (encap), an encapsulation/organization type (orga/encap) and organization type (orga).

Fig.10 Remaining particle material (coral and ceramic bone). a; 2 weeks after implantation of particles (large group, medium group, and small group). b; 4 weeks, c; 6 weeks, d; 8 weeks, e; 12 weeks * Differences of $P<0.05$ were considered significant.

After 6 weeks, the organization type was more common in the large (75.0%), medium (66.7%), and small (100%) groups of the coral experimental group. Particle clusters were fractured into sections, and many foreign body giant cells were observed on the particle surfaces and interconnection pathways. Reduction of the area of the remaining particle clusters was seen, and there were cases of complete disappearance in the medium (25.0%) and small (25.0%) groups (Figs. 6a, 6b, 6c, 9, 10, 11). In the ceramic bone experimental group, the organization type also increased in the large (57.1%), medium (85.7%), and small (83.3%) groups, and many foreign body giant cells were observed in the particle interconnection pathways, but there were no cases of complete disappearance (Figs. 6d, 6e, 6f, 9, 10, 11). The number of cases with reduction of the area or complete disappearance of particles statistically increased in large, medium, and small coral groups of the coral group compared with the respective ceramic bone group (*P*<0.05) (Fig. 10).

After 8 weeks, the organization type was seen in all cases of the coral experimental group, and the particle clusters were replaced by fibrous connective tissue consisting mainly of collagen fibers. There were a number of cases in which complete disappearance increased in the large (33.3%), medium (50.0%), and small (80.0%) groups (Figs. 7a, 7b, 7c, 9, 10, 11). In the ceramic bone experimental group, nearly all cases were organization type. Foreign body giant cells increased in the interconnection pathways and reduction in the area of the remaining particles was seen. However, there were no cases with complete disappearance in the large, medium and small groups (Figs. 7d, 7e, 7f, 9, 10, 11). The number of cases with reduction of the area of the remaining particles and complete dis-
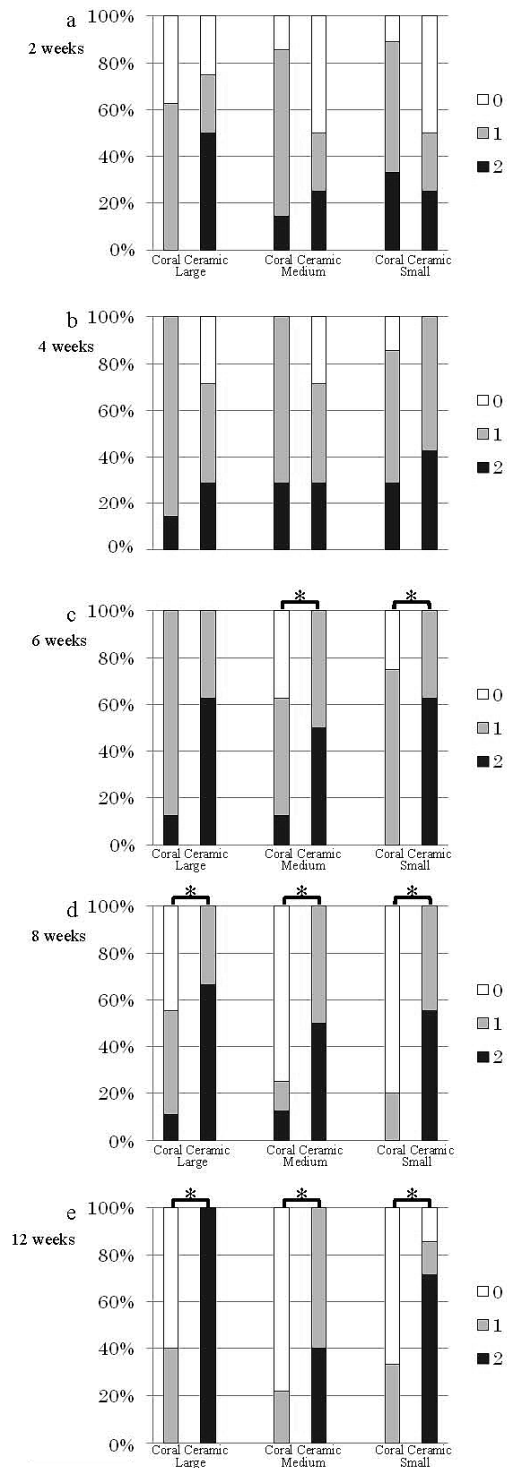

Fig.11 Infiltration of foreign body giant cells (coral and bioceramic bone). a; 2 weeks after implantation of particles (large group, medium group, and small group). b; 4 weeks, c; 6 weeks, d; 8 weeks, e; 12 weeks * Differences of P<0.05 were considered significant.

appearance statistically increased in the large, medium, and small groups of coral group compared with the respective ceramic bone experimental group (*P*<0.05) (Fig. 10).

After 12 weeks, many cases in which complete disappearance of particles had been observed in the large (70.0%) medium (77.8%) and small (88.9%) groups showed replacement with well-developed collagen fibers (scarring) and disappearance of macrophages and foreign body giant cells (Figs. 8a, 8b, 8c, 9, 10, 11). In the ceramic bone experimental group, all cases were the organization type and particle cluster area reduction was seen, with some cases of complete disappearance in the small group (14.2%). However, there were no cases of complete disappearance in the medium or large groups (Figs. 8d, 8e, 8f, 9, 10, 11). The number of cases with reduction of the area of the remaining particles and complete disappearance statistically increased in the large, medium, and small groups of coral group compared with the respective ceramic bone experimental group (*P*<0.05) (Fig. 10).

DISCUSSION

The internal structure of coral has been shown to be porous with numerous tubes of 50–300 μm diameter. Its exoskeleton surface is covered with rough elevations. The internal structure of ceramic bone is porous with spherical pores of 100–200 μm. Porosity increases the surface area of a substance and is suitable for cell proliferation. Considering cell size, a pore size of ≥10 μm is needed. In the formation of capillaries, pore sizes of ≥100 μm are ideal, while in bone formation pore sizes of 50–250 μm are ideal[14]. This kind of cell proliferation cannot be expected with pore sizes of ≤10 μm, but such materials implanted in the body can be applied as drug delivery systems for bone growth

factors such as fibroblast growth factor (FGF) and bone morphogenetic protein (BMP) [20, 21].

In the formation of new bone, the surface structure of substances in contact with cells should ideally be rough. Greater induction of newly formed bone can be expected with rough than smooth titanium surfaces in the jaw, and for that reason acid-etching or sand blasting is used to give roughness to the surfaces of dental implants [22]. Thus, cell proliferation and differentiation can be expected with the rough surface of coral. The surface of the coral exoskeletons used in this study was covered with innumerable rough protuberances of 10–20 μm. The surface of the ceramic bone was smoother than that of the rough coral.

Physical strength is needed in scaffolding material for bone augmentation. The compressive strength of the coral (64.3 MPa) was greater than that of the ceramic bone (44.8 MPa). Moreover, the strength of the both coral and ceramic bone was greater than that of human cancellous bone (2-7 MPa) [23] or β-TCP (2-3 MPa) [24]. It was thought that both coral and ceramic bone were useful scaffold for bone augmentation. In places distant from the added particles of coral or ceramic bone, the co-culture cell number was smaller than in the control group. However, increases in cell number were seen in places of contact with these particles. From this it is thought that coral and ceramic bone have tissue affinity, and induce cell proliferation.

Similarly, in places separated from these particles there was little capillary formation, while much formation was observed in contact with the particles. Nishikawa *et al*. (2011) [25] described the chemical features of coral, in which calcium ions of coral particles are released in acidic solutions, while in alkaline solutions calcium ions in the solution are

deposited on the surface of the particles. Calcium ions are needed in the differentiation of vascular endothelial cells into capillaries [26], and in culture solution with added coral particles the calcium concentration decreases in places distant from the particles, whereas the calcium concentration might be high near the particles or in places contacting the particles. Thus, it is thought that differentiation into capillaries was induced near the particles. Capillaries are a component of the granulation tissue which is necessary to process the scaffold and to form new bone.

When large, medium, and small particles of coral and ceramic bone were implanted into rat subcutaneous tissue, capillary proliferation, macrophage and lymphocyte infiltration around particle clusters, and encapsulation by granulation tissue were seen at 2 weeks after implantation. Foreign bodies smaller than about 3 μm are phagocytosed by neutrophils, and those smaller than about 10 μm are phagocytosed by macrophages [27, 28]. The lymphocyte infiltration in these coral and ceramic bone particles was not strong. Thus, the particle processing seems to be non-specific phagocytosis, so that there would be no allergic reaction with use of these materials as a scaffold [29]. At 4 weeks after implantation, there were many cases of organization type with invasion of granulation tissue and fractioning of particle clusters in the coral group, and many cases of encapsulation type with the particle clusters enclosed by granulation tissue in the large and medium of ceramic bone group. A greater decrease in the area of particle clusters was seen in the organization type than in the encapsulation type. From 4 to 6 weeks, foreign body giant cells appeared on the surface and in interconnection pathways of particles in the coral and ceramic bone experimental groups. These are foreign body giant cells that form fused macrophages in response to foreign bodies larger than macrophages [30], and they are thought to have phagocytosed the particles, which are resolved by nitric oxide in macrophages [31]. From 8 to 12 weeks after implantation, the area of particle clusters decreased in the coral group, and at the same time the diameter of particles phagocytosed by foreign body giant cells became smaller. There were many cases of complete particle disappearance in the coral group, and replacement with fibrous connective tissue containing mild capillary formation. In the ceramic bone group, there were cases in which particles disappeared in the small particle group, but none in the medium or large groups. The above demonstrates that coral particles are easier for the host to process than ceramic bone.

CONCLUSIONS

This study of the histological reaction to porous coral and ceramic bone as a scaffold material revealed the following. 1. Coral has a porous structure with pore size of 50–300 μm; ceramic bone also has a porous structure, with pore sizes of 100–200 μm. 2. Both coral and ceramic bone have tissue affinity and induce cell proliferation and capillary differentiation. 3. Both coral and ceramic bone are bioabsorbable with granulation tissue, and particles of these materials are phagocytosed by foreign body giant cells. 4. The time for disappearance of particles is shorter with coral particles than with ceramic bone particles.

ACKNOWLEDGMENTS

REFERENCES

1) Doll B, Sfeir C, Winn S, Huard J, Hollinger J. Critical aspects of tissue-engineered therapy for bone regeneration. Crit Rev Eukaryot Gene Expr 2001;11:173-198.
2) Ulery BD, Nair LS, Laurencin CT. Biomedical applications of biodegradable polymers. J Polym Sci B: Polym Phys 2011; 49:832-864.
3) Heinemann S, Gelinsky M, Worch H, Hanke T. Resorbable bone substitution materials: An overview of commercially available materials and new approaches in the field of composites. Orthopade 2011;40:761-773.
4) Cricchio G, Palma VC, Faria PE, de Olivera JA, Lundgren S, Sennerby L, Salata LA. Histological outcomes on the development of new space-making devices for maxillary sinus floor augmentation. Clin Implant Dent Relat Res 2011;13:224-230.
5) Jannetty J, Kolb E, Boxberger J, Deslauriers R, Ganey T. Guiding bone formation in a critical-sized defect and assessments. J Craniofac Surg 2010; 21:1848-1854.
6) Fennis JP, Stoelinga PJ, Jansen JA. Mandibular reconstruction: A clinical and radiographic animal study on the use of autogenous scaffolds and platelet-rich plasma. Int J Oral Maxillofac Surg 2002;31:281-286.
7) Sbordone C, Toti P, Guidetti F, Califano L, Santoro A, Sbordone L. Volume changes of iliac crest autogenous bone grafts after vertical and horizontal alveolar ridge augmentation of atrophic maxillas and mandibles: A 6-year computerized tomographic follow-up. J Oral Maxillofac Surg 2012;70:2559-2565.
8) Damien CJ, Parsons JR. Bone graft and bone graft substitutes: A review of current technology and applications. J Appl Biomater 1991;2:187-208.
9) Finkemeier CG. Bone-grafting and bone-graft substitutes. J Bone Joint Surg Am 2002;84:454-464.
10) Gérard C, Doillon CJ. Facilitating tissue infiltration and angiogenesis in a tubular collagen scaffold. J Biomed Mater Res A 2010;93:615-624.
11) Liao SS, Cui FZ, Zhang W, Feng QL. Hierarchically biomimetic bone scaffold materials: Nano-HA/collagen/PLA composite. J Biomed Mater Res B Appl Biomater 2004;15;69:158-165.
12) Rokn A, Moslemi N, Eslami B, Abadi HK, Paknejad M. Histologic evaluation of bone healing following application of anorganization bovine bone and β-tricalcium phosphate in rabbit calvaria J Dent (Tehran) 2012;9:35-40.
13) Lin CY, Kikuchi N, Hollister SJ. A novel method for biomaterial scaffold internal architecture design to match bone elastic properties with desired porosity. J Biomech 2004;37:623-636.
14) Karageorgiou V, Kaplan D. Porosity of 3D biomaterial scaffolds and osteogenesis. Biomaterials 2005;26:5474-5491.
15) Jung UW, Hwang JW, Choi DY, Hu KS, Kwon MK, Choi SH, Kim HJ. Surface characteristics of a novel hydroxyapatite-coated dental implant. J Periodontal Implant Sci 2012;42:59-63.
16) Feng YF, Wang L, Li X, Ma ZS, Zhang Y, Zhang ZY, Lei W. Influence of architecture of β-tricalcium phosphate scaffolds on biological performance in repairing segmental bone defects. PLOS One 2012;7:1-12.
17) Mastrogiacomo M, Scaglione S, Martinetti R, Dolcini L, Beltrame F, Cancedda R, Quarto R. Role of scaffold internal structure on in vivo bone formation in macroporous calcium phosphate bioceramics. Biomaterials 2006;27:3230-3237.
18) Nishikawa T, Masuno K, Tominaga K, Koyama Y, Yamada T, Takakuda K, Kikuchi M, Tanaka J, Tanaka A. Bone repair analysis in a novel biodegradable hydroxyapatite/collagen composite implanted in bone. Implant Dent 2005;14: 252-260.
19) Zhang JC, Lu HY, Lv GY, Mo AC, Yan YG, Huang C. The repair of critical-size defects with porous hydroxyapatite/polyamide nanocomposite: an experimental study in rabbit mandibles. Int J Oral Maxillofac Surg 2010;39:469-477.
20) Elsner JJ, Zilberman M. Antibiotic-eluting bioresorbable composite fibers for wound healing applications: microstructure, drug delivery and mechanical properties. Acta Biomater 2009;5:2872-2883.
21) Luong LN, Ramaswamy J, Kohn DH. Effects of osteogenic growth factors on bone marrow stromal cell differentiation in a mineral-based delivery system. Biomaterials 2012;33:283-294.
22) Onur MA, Sezgin A, Gürpinar A, Sommer A, Akça K, Cehreli M. Neural response to sandblasted/acid-etched, TiO-blasted, polished, and mechanochemically polished/nanostructured ti-

tanium implant surfaces. Clin Oral Implants Res 2006;17:541-547.

23) Lotz JC, Gerhart TN, Hayes WC. Mechanical properties of trabecular bone from the proximal femur: a quantitative CT study. J Comput Assist Tomogr 1990;14:107-114.

24) Zhao XF, Li XD, Kang YQ, Yuan Q. Improved biocompatibility of novel poly(L-lactic acid)/β-tricalcium phosphate scaffolds prepared by an organization solvent-free method. Int J Nanomedicine 2011;6:1385-1390.

25) Nishikawa T, Okamura T, Masuno K, Tominaga K, Wato M, Uobe K, Imai K, Takeda S, Kono T, Morita S, Hidaka M, Tanaka A. Tissue affinity and chemical characteristics of coral. Nano Biomedicine 2011;3;231-236.

26) Shen WG, Peng WX, Dai G, Xu JF, Zhang Y, Li CJ. Calmodulin is essential for angiogenesis in response to hypoxic stress in endothelial cells. Cell Biol Int 2007;31:126-134.

27) Kumazawa R, Watari F, Takashi N, Tanimura Y, Uo M, Totsuka Y. Effects of Ti ions and particles on neutrophil function and morphology. Biomaterials 2002;23:3757-3764.

28) Panilaitis B, Altman GH, Chen J, Jin HJ, Karageorgiou V, Kaplan DL. Macrophage responses to silk. Biomaterials 2003;24:3079-3085.

29) Ghani S, Feuerer M, Doebis C, Lauer U, Loddenkemper C, Huehn J, Hamann A, Syrbe U. T cells as pioneers: antigen-specific T cells condition inflamed sites for high-rate antigen-non-specific effector cell recruitment. Immunology 2009; 128:e870-880.

30) Brodbeck WG, Anderson JM. Giant cell formation and function. Curr Opin Hematol 2009;16:53-57.

31) Vazquez-Torres A, Stevanin T, Jones-Carson J, Castor M, Read RC, Fang FC. Analysis of nitric oxide-dependent antimicrobial actions in macrophages and mice. Methods Enzymol 2008;437:521-538.

Corresponding author:
Ono Takanao, DDS
Department of Orthodontics, Osaka Dental University
8-1 Kuzuhahanazono-cho, Hirakata, Osaka 573-1121, Japan
Tel:+81-72-864-3078
Fax:+81-72-864-3178
E-mail: taka-ono@cc.osaka-dent.ac.jp